

# Synthesis of nanocellulose derived from oil palm empty fruit bunch cellulose via the ultrasound method

Khairiyah Qanitah<sup>1\*</sup>, Nugraha Edhi Suyatma<sup>1</sup>, Saraswati<sup>1</sup>, and Sri Yuliani<sup>2</sup>

<sup>1</sup>Department of Food Science and Technology, IPB University, Bogor, Indonesia

<sup>2</sup>Research Center for Agroindustry, National Research and Innovation Agency, Tangerang Selatan, Indonesia

**Abstract.** Oil palm is a major plantation in Indonesia, producing significant waste like oil palm empty fruit bunches (OPEFBs). For every ton of crude palm oil, 1.1 tons of waste are generated. OPEFBs, rich in cellulose, are promising raw materials for nanocellulose production, which has valuable applications in food, cosmetics, and biomedicine. This study investigated nanocellulose production using an ultrasound method (Ultrasonic FS, 300 W), a green and cost-effective technology. The research explored the impact of ultrasonic treatment duration (30, 60, and 90 minutes) on nanocellulose's structure and properties. Nanocellulose was produced from microfibre cellulose derived from OPEFBs. High-resolution transmission electron microscopy (HR-TEM) was used to assess morphology, average diameter, and diameter distribution, while Fourier transform infrared (FT-IR) spectroscopy analysed total crystalline index (TCI), lateral order index (LOI), and hydrogen bond intensity (HBI). Results showed that nano-dimensioned cellulose fibres were observed, and 60 minutes of ultrasonic treatment was optimal, yielding nanocellulose with an average diameter of  $8.939 \pm 0.714$  nm and a diameter distribution of 1-60 nm. While ultrasonic treatment did not significantly affect the TCI value (from 1.0769 to 1.0915), it slightly altered the chemical composition, as indicated by spectral patterns at wavenumbers  $3300\text{ cm}^{-1}$  and  $1427\text{ cm}^{-1}$ , showing increased intensity of OH-stretch and CH<sub>2</sub> bond (corresponding to the cellulose crystallinity band), correlating with increased HBI (from 0.5890 to 0.9754) and LOI values (from 0.9792 to 1.1394). Thus, the ultrasound method proved to be a promising and efficient approach for synthesizing nanocellulose.

## 1 Introduction

Oil palm is one of the largest plantation sectors in Indonesia that produces palm oil and palm kernel oil, which are much needed by industry. The volume of palm oil production in Indonesia reached 48.235 million tons in 2022 [1]. This makes Indonesia the largest palm oil-producing country in the world. The world palm oil production in 2023 reached 79.464 million metric tons and Indonesia produced 47 million metric tons, or around 59% of palm oil production worldwide [2]. Every ton of crude palm oil production will produce 1.1 tons of oil palm empty fruit bunches (OPEFBs) waste [3]. OPEFBs could be developed as a raw material for making nanocellulose. The most significant chemical composition of OPEFBs is cellulose, around 53.37%, and contains 19.88% hemicellulose and 10.74% lignin [4].

Cellulose is a biopolymer consisting of  $\beta$ -D-glucopyranose units linked by  $\beta$ -1,4 glycosidic bonds. Nanocellulose is a nano-sized cellulose material with a diameter of less than 100 nm and a length of less than 1000 nm. This nano-size produces different characteristics compared to cellulose. Nanocellulose has many beneficial physical and chemical properties,

including a large specific surface area and aspect ratio, strong mechanical properties like high tensile strength, modulus, and stiffness, good optical properties, biocompatibility, and biodegradability [5]. Besides, cellulose is non-toxic and environmentally friendly, with a high natural abundance [6]. Therefore, nanocellulose is a fascinating material for application in many fields. Numerous studies have explored the applications of nanocellulose, including its role as a nanofiller in polymer nanocomposites, a Pickering stabilizer in food emulsions, a packaging enhancer, a thickening agent in cosmetics, and a material for drug delivery, tissue engineering, and wound healing in biomedical fields [5, 7-9].

Nanocellulose can be obtained using several processes, specifically top-down and bottom-up approaches. The top-down process involves reducing the size of materials to create nanostructures. In contrast, the bottom-up method involves arranging atoms or molecules and combining them through chemical reactions to generate nanostructures. An example of a bottom-up approach is using sol-gel technique, precipitation chemistry, and gas phase agglomeration. Meanwhile, the top-down approach includes grinding with milling, homogenization techniques, ultrasonic,

\* Corresponding author: [khairiyahqanitah@apps.ipb.ac.id](mailto:khairiyahqanitah@apps.ipb.ac.id)

micro-fluidization, etc. [10]. The type of raw materials used, their pretreatment, and the disintegration process determine which of these approaches produces a distinct kind of nanocellulose [11].

Typically, nanofibre cellulose (NFC) is obtained through mechanical processing following chemical or enzymatic pretreatment in cellulose production [12-14]. The cellulose fibre is subsequently downsized to synthesize nanocellulose through high-shear mechanical techniques, including high-pressure homogenization, grinding or milling, cryo-crushing, high-intensity ultrasonics, and micro-fluidization [3, 8, 15-17]. Compared to other methods, the ultrasonic approach is a more environmentally friendly and highly efficient technology for nanocellulose production. This method not only reduces energy consumption but also minimizes chemical usage, making it a sustainable alternative for large-scale production [5, 18].

The isolation of NFC from OPEFBs has been reported using several techniques, such as a combination of ultrafine grinding and ultrasonication [19], nano-grinding [17] and a combination of TEMPO oxidation and microfluidization [20]. To the best of our knowledge, there are few reports on the precise use of ultrasound for synthesizing NFC derived specially from OPEFBs cellulose.

Hence, this study aimed to synthesize and characterize NFC derived from microfibre cellulose (MFC) of OPEFBs through ultrasonic method. The nanocellulose obtained was characterized in terms of its morphology, average diameter, and diameter distribution using HR-TEM and total crystalline index (TCI), lateral order index (LOI), and hydrogen bond intensity (HBI) using FT-IR spectroscopy.

## 2 Materials and Method

### 2.1 Production of Nanocellulose

In order to produce nanocellulose, MFC of OPEFBs was obtained from PT Mandiri Palmera Agrindo (Indonesia). First, the sample was sieved using a 100-mesh sieve and then dispersed in deionized water with a concentration of 2.5% w/v. Next, the suspension was ultrasonicated using an Ultrasonic processor (FS 300, China) operated at a frequency of 20 kHz with a maximum power of 300 W, 90% amplitude, and the pulse mode was set on/off for 3 seconds with varying periods (30, 60, and 90 minutes). The nanocellulose suspension was then dried using a spray dryer SD-BASIC (LabPlant, UK) at an inlet temperature of 170 °C and an outlet temperature of 90°C for FT-IR spectroscopy analysis. In contrast, for HR-TEM analysis, the nanocellulose was characterized in its suspension form to preserve its native nanostructure.

### 2.2 Characterization of Nanocellulose

Morphological analysis of nanocellulose was carried out using a high-resolution transmission electron microscopy (HR-TEM) instrument (Talos F200C G2, USA). First, the samples were prepared by diluting it 100 times with Millipore water and then stained with 2% uranyl acetate for 2 minutes. Next, the sample was placed on a 200-mesh copper grid, and then the grid was mounted into the instrument tube for visualisation.

Diameter analysis of nanocellulose was measured using ImageJ software. The images from the HR-TEM instrument were used for diameter analysis. Briefly, the known distance, distance in pixels, and unit of scale were inserted, and the diameter was measured randomly for each image. After that, the diameter distribution was analysed using Origin 2024 (OriginLab, USA).

Fourier transform infrared (FT-IR) spectroscopy was conducted using the FT-IR Prestige 21 instrument (Shimadzu, Japan) to analyse MFC and nanofiber cellulose after 60 minutes of ultrasonic treatment (NFC-60). Samples were mixed with potassium bromide (KBr) and placed onto a sample holder, followed by compression to form pellets. Then, a scanning process was carried out on the sample with a wave number of 4000-400  $\text{cm}^{-1}$ . Three different measurements for each fiber were evaluated, and the average value was considered. Total crystalline index (TCI), lateral order index (LOI), and hydrogen bond intensity (HBI) were assessed for each sample following Poletto et al. [21] methods. TCI value is the ratio between the absorbance band at 1372 and 2900  $\text{cm}^{-1}$ , LOI value is the ratio of the absorbance band at 1429 and 897  $\text{cm}^{-1}$ , and HBI value is the ratio of the absorbance band at 3400  $\text{cm}^{-1}$  and 1320  $\text{cm}^{-1}$ . The measurement was performed in duplicate, and the data was statistically analysed using an independent sample t-test by Microsoft Excel software.

## 3. Results and Discussion

The morphology of nanocellulose derived from OPEFBs under different ultrasonic durations was investigated using high-resolution transmission electron microscopy (HR-TEM). As shown in Figure 1, the nanocellulose exhibited long, entangled fibril structures. Increasing the ultrasonic duration led to the gradual breakdown of the cellulose fibrils into smaller fragments, forming small chunks and needle-like structures. Similarly, Peng et al. [22] reported that NFC exhibited needle-like fibril shapes and large cell wall sections (chunks). However, after 90 minutes of ultrasonic treatment, the fibrils tended to re-aggregate into larger chunks, consistent with the size distribution results (Figure 2a).

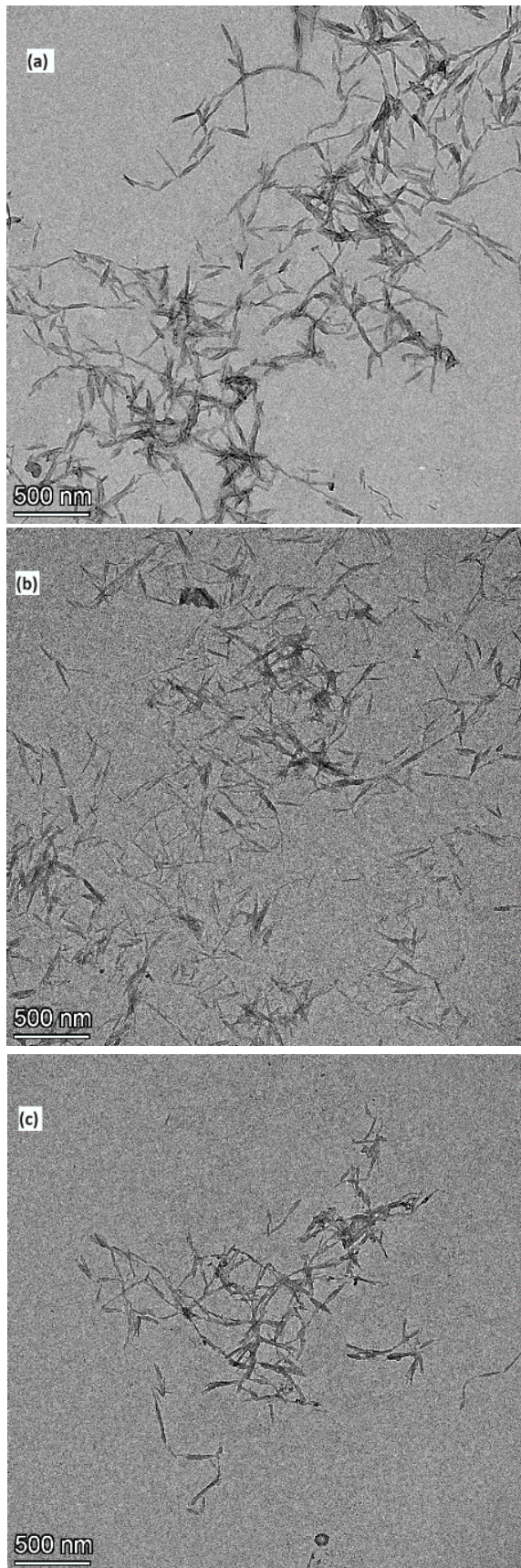


**Figure 1** HR-TEM micrographs at 17500x magnification of dispersed nanocellulose at different ultrasonic times: 30 min (a), 60 min (b), and 90 min (c)

The size of the cellulose decreased with increasing ultrasonic time due to the effects of acoustic cavitation. During cavitation, the potential energy of expanding bubbles is converted into the kinetic energy of liquid jets. These jets travel through the bubbles, penetrate the opposite bubble wall at several hundred meters per second, and hit the surface of the cellulose, causing bond breakages that gradually disintegrate the micron-sized cellulose into nanocellulose [23]. Nonetheless, as the size of NFC decreased, it tended to aggregate more readily due to a reduction in exposed surface charges (NFC had more charges because of its larger specific surface area) and a subsequent decrease in zeta potential [15].

Figure 2 presents the average diameter and diameter distribution of nanocellulose under different ultrasonic treatment durations. The data indicate that particle size decreased as the ultrasonic time increased from 30 to 60 minutes, reducing the average diameter from  $34,616 \pm 0,761$  nm to  $8,939 \pm 0,714$  nm, and the diameter distribution of nanocellulose after 30 minutes of treatment ranged from 7-200 nm, and after 60 minutes of treatment ranged from 1-60 nm, respectively. However, prolonging the duration of ultrasonic treatment promoted agglomeration. As shown in Figure 2, after 90 minutes of ultrasonic treatment, the average diameter increased to  $26,529 \pm 0,741$  nm, and the diameter distribution increased to 7-140 nm.

The cavitation effect generated during ultrasonication disrupts the hydrogen bonds predominantly linking the cellulose fibres. This phenomenon occurs as cavitation produces microbubbles that rapidly oscillate and collapse, generating shock waves and localized high-pressure conditions. As a result, the relatively weak inter-fibrillar hydrogen bonds are broken, leading to the gradual disintegration of micron-sized cellulose fibres into nanofibers [11]. However, extending the ultrasonic treatment increased the number of hydroxyl groups on the NFC surface. The abundance of hydroxyl groups promoted aggregation and facilitated the formation of strong new hydrogen bonds between adjacent fibres [24].

Similar findings were reported by Fahma et al. [19] that NFC isolated from OPEFBs using mechanical treatment (a combination of ultrafine grinding and ultrasonication) has a diameter of  $33.62 \pm 6.8$  nm. Extending ultrasonic treatment encouraged the formation of chitin nanofibre agglomerates. During sonication, three steps were observed: deagglomeration, re-agglomeration, and deagglomeration [10]. Therefore, duration of ultrasonication is believed to play a significant role in NFC morphology and size distribution. Producing nanocellulose from OPEFBs using the ultrasonication method is feasible and practical.

FT-IR spectroscopy evaluated the effect of ultrasonication on chemical composition. The spectra of MFC and NFC-60 are shown in Figure 3. The patterns are slightly different. Based on the data, there are a slight change in infrared spectra during ultrasonication treatment. Following the sonication treatment (NFC-

60), a distinct peak emerges, particularly at wavelengths of  $3300\text{ cm}^{-1}$  and  $1427\text{ cm}^{-1}$ . O-H stretching, a characteristic of type I cellulose, is responsible for peaks between  $4000\text{--}2995\text{ cm}^{-1}$  [3, 25]. Based on the data, the absorption of O-H groups increased after ultrasonic treatment. The increase in O-H groups is attributed to the cavitation effect generated during the ultrasonication process, which disrupts hydrogen bonds between fibrils and enhances the number of hydroxyl groups in the sample [11]. The peak  $1420\text{--}1430\text{ cm}^{-1}$  was assigned to the  $\text{CH}_2$  bond in cellulose, which corresponded to the cellulose crystallinity band. Based on the data, the absorption of  $\text{CH}_2$  (corresponding to cellulose crystallinity) increased after ultrasonic treatment [13, 15]. This increase indicates that during ultrasonication, the cavitation effect is likely to influence the structure of cellulose. This finding is further supported by the infrared crystallinity ratio analysis presented in Table 1.

Apart from the two wavelengths mentioned above, the band patterns obtained from both samples are nearly identical. Several functional groups that can be identified are as follows: The peak at  $2900\text{ cm}^{-1}$  represented the C-H symmetric stretching vibration [12]. The band  $902\text{--}893\text{ cm}^{-1}$  is associated with  $\beta$ -glycosidic linkages between glucose units, which are correlated to the amorphous band. The  $1750\text{--}1735\text{ cm}^{-1}$  peak is linked to the acetyl and uronic ester groups' C=O stretching vibration. These groups are found in pectin, hemicellulose, and lignin [26]. The peak at  $1519\text{ cm}^{-1}$  assigned to aromatic rings, suggesting the presence of lignin [15]. However, both samples showed no such peak, suggesting complete removal of lignin.

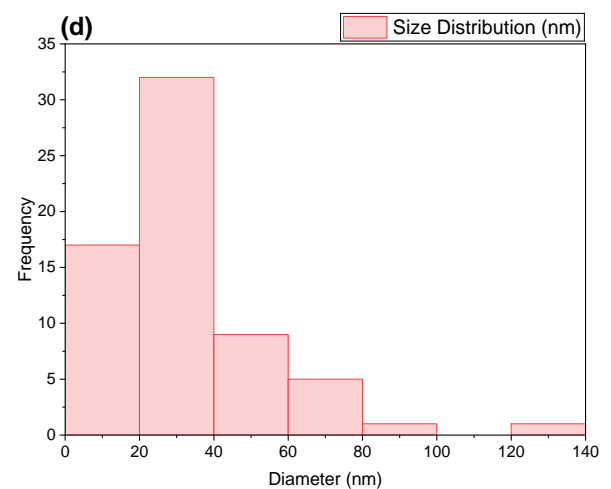
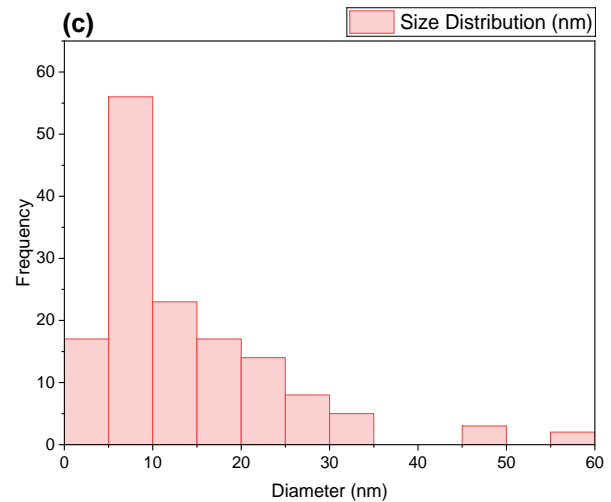
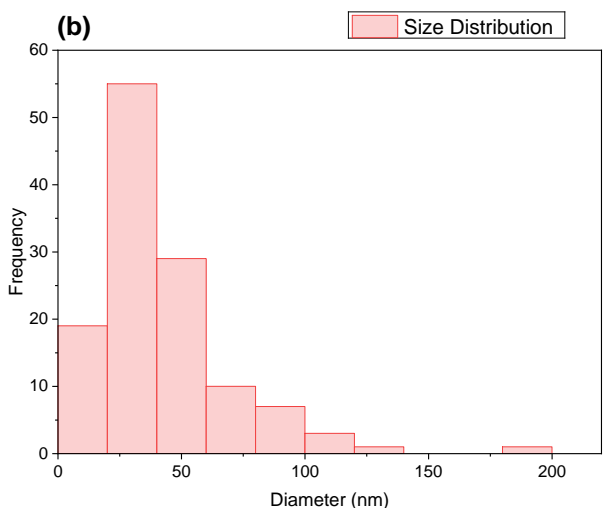
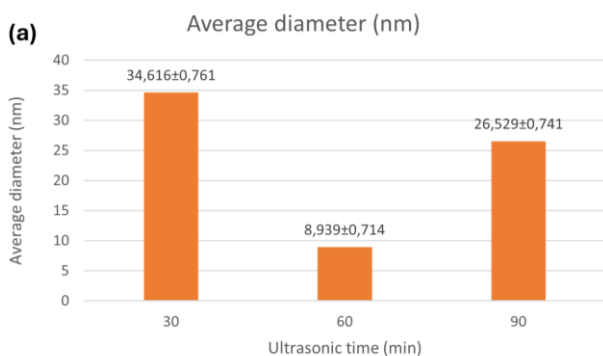


**Figure 2** The average diameter (a), The diameter distribution of nanocellulose at different ultrasonic durations: 30 min (b), 60 min (c), and 90 min (d)

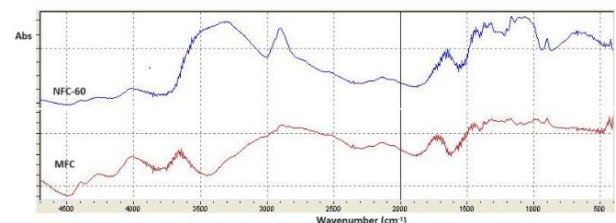


**Figure 3** FT-IR spectra of microfibrillar cellulose (MFC) & Nanocellulose after 60 min ultrasonication (NFC-60)

The infrared crystallinity ratio could estimate the crystallinity of cellulose after ultrasonic treatment. The crystalline structure of cellulose is associated with the band around  $1420\text{--}1430\text{ cm}^{-1}$  while the amorphous region in cellulose corresponds to the band at  $898\text{ cm}^{-1}$  [27]. The ratio of these two bands, defined as the lateral order index (LOI), serves as an empirical crystallinity index. Additionally, the ratio of the bands at  $1372$  and  $2900\text{ cm}^{-1}$  is the total crystalline index (TCI). The TCI value is associated with the crystallinity degree of cellulose, while the LOI value is proportional to the overall degree of order in cellulose [21]. Hydrogen bond intensity (HBI), defined as the ratio between the absorbance bands at  $3400\text{ cm}^{-1}$  and  $1320\text{ cm}^{-1}$ , is another

measurement that correlates to qualitative changes in the crystallinity of cellulose. The HBI value is significantly influenced by chain mobility and bond distance. It is closely associated with the crystal structure, the degree of intermolecular organization (crystallinity), and the amount of bound water [28].

**Table 1** Infrared crystallinity ratio and hydrogen bond intensity of the microfibre cellulose (MFC) and Nanocellulose after 60 min ultrasonication (NFC-60)

Sample	IR crystallinity ratio		HBI A3400/A1 320
	A1372/A2900 (TCI)	A1429/A897 (LOI)	
MFC	1,0769 <sup>a</sup>	0,9792 <sup>a</sup>	0,5890 <sup>a</sup>
NFC- 60	1,0915 <sup>a</sup>	1,1394 <sup>b</sup>	0,9754 <sup>b</sup>

Different superscript letters in the same column indicate significantly different according to the t-test ( $p < 0,05$ )

The infrared crystallinity ratio and hydrogen bond intensity of microfibre cellulose (MFC) and nanocellulose after 60 minutes of ultrasonication are shown in Table 1. The LOI values obtained from this study are 0,9792 and 1,394. The HBI values recorded in this study are 0,5890 and 0,9754, and the TCI values are 1,0769 and 1,0915. Based on the data, the TCI value showed no significant impact on ultrasonic treatment. However, the LOI and HBI values increased slightly after ultrasonication. This indicating that the ultrasonic treatment did not change the overall degree of crystallinity. However, it slightly increased its ordered structure. The rise in HBI indicated that more hydroxyl groups became available for forming inter- and intramolecular hydrogen bonds within the sample [29]. This increase was likely attributed to the cavitation effect produced by ultrasonication, which caused the disruption of inter-fibrillar hydrogen bonds and raised the number of hydroxyl groups in the sample [11]. Previous study reported that ultrasonication decreased the hydrogen bond distance in pure cellulose, promoting the alignment of linear glucose chains and, thereby, enhancing crystallization [30].

## 4 Conclusion

The ultrasound method has been successful in synthesizing nanocellulose from OPEFBs. Morphology analysis confirmed that nano-dimensioned cellulose fibres were observed, and 60 minutes of ultrasonic treatment is optimal, resulting in an average diameter of  $8.939 \pm 0.714$  nm and a diameter distribution of 1-60 nm. Ultrasonic treatment did not significantly impact on the total crystalline index (TCI). However, it had a slight effect on the chemical composition, as confirmed by the spectral patterns at wavenumbers  $3300\text{ cm}^{-1}$  and  $1427\text{ cm}^{-1}$ , showing the increased intensity of OH-stretch and  $\text{CH}_2$  bond (corresponding to the cellulose crystallinity band), correlating with increased HBI and LOI values after 60 minutes of ultrasonic treatment. Based on the characterization data, the ultrasound method is a promising and efficient treatment for synthesizing nanocellulose from microfibre cellulose of OPEFBs.

Acknowledgements: The authors are grateful for the financial support provided by Indonesia Endowment Fund for Education (LPDP) from the Ministry of Finance Republic Indonesia.

## References

- [1] Directorate General of Plantations Ministry of Agriculture, "Statistik Perkebunan Unggulan Nasional 2020-2022," 2022. Accessed: Aug. 28, 2023. [Online]. Available: <https://repository.pertanian.go.id/items/529921cc-7268-49f7-ae70-c44c74271a6f>
- [2] USDA, "Palm Oil Explorer." Accessed: Aug. 05, 2023. [Online]. Available: <https://ipad.fas.usda.gov/cropexplorer/cropview/commodityView.aspx?cropid=4243000>
- [3] F. Fahma, S. Iwamoto, N. Hori, T. Iwata, and A. Takemura, Isolation, preparation, and characterization of nanofibers from oil palm empty-fruit-bunch (OPEFB), *Cellulose*, vol. **17**, no. 5, pp. 977–985 (2010) <https://doi.org/10.1007/s10570-010-9436-4>
- [4] Z. Ibrahim, M. Ahmad, A. A. Aziz, R. Ramli, K. Hassan, and A. H. Alias, Properties of chemically treated oil palm empty fruit bunch (efb) fibres, *J of Adv Rsc in Fluid Mech and Therm Sci*, vol. **57**, pp. 57–68 (2019)
- [5] Q. Ji, C. Zhou, Z. Li, I. D. Boateng, and X. Liu, Is nanocellulose a good substitute for non-renewable raw materials? a comprehensive review of the state of the art, preparations, and industrial applications, *Ind Crops Prod*, vol. **202**, p. 117093, (2023). <https://doi.org/10.1016/j.indcrop.2023.117093>
- [6] F. Zhang, R. Shen, N. Li, X. Yang, and D. Lin, Nanocellulose: An amazing nanomaterial with diverse applications in food science, *Carbohydr Polym*, vol. **304** (2023). <https://doi.org/10.1016/j.carbpol.2022.120497>
- [7] S. Roy and J. W. Rhim, Gelatin/agar-based functional film integrated with Pickering emulsion of clove essential oil stabilized with nanocellulose for active packaging applications, *Colloids Surf A Physicochem Eng Asp*, vol. **627** (2021). <https://doi.org/10.1016/j.colsurfa.2021.127220>
- [8] M. L. Foo, C. W. Ooi, K. W. Tan, and I. M. L. Chew, Preparation of black cumin seed oil Pickering nanoemulsion with enhanced stability and antioxidant potential using nanocrystalline cellulose from oil palm empty fruit bunch, *Chemosphere*, vol. **287** (2022). <https://doi.org/10.1016/j.chemosphere.2021.132108>
- [9] M. Amrani, S. Pourshamohammad, M. Tabibiazar, H. Hamishehkar, and M. Mahmoudzadeh, Antimicrobial activity and

- stability of *Satureja khuzestanica* essential oil pickering emulsions stabilized by starch nanocrystals and bacterial cellulose nanofibers, *Food Biosci*, vol. **55**, p. 103016 (2023).  
<https://doi.org/10.1016/j.fbio.2023.103016>
- [10] H. Zou, B. Lin, C. Xu, M. Lin, and W. Zhan, Preparation and characterization of individual chitin nanofibers with high stability from chitin gels by low-intensity ultrasonication for antibacterial finishing, *Cellulose*, vol. **25**, no. 2, pp. 999–1010 (2018).  
<https://doi.org/10.1007/s10570-017-1634-x>
- [11] W. Chen, H. Yu, Y. Liu, P. Chen, M. Zhang, and Y. Hai, Individualization of cellulose nanofibers from wood using high-intensity ultrasonication combined with chemical pretreatments, *Carbohydr Polym*, vol. **83**, no. 4, pp. 1804–1811 (2011).  
<https://doi.org/10.1016/j.carbpol.2010.10.040>
- [12] J. Wang *et al.*, Preparation of nanocellulose in high yield via chemi-mechanical synergy, *Carbohydr Polym*, vol. **251** (2021).  
<https://doi.org/10.1016/j.carbpol.2020.117094>
- [13] N. I. Abdo, Y. M. Tufik, and S. M. Abobakr, A comparison of nano-celluloses prepared with various terms of time and sulfuric acid concentration from bagasse derived cellulose: Physicochemical characteristics and process optimization, *Current Research in Green and Sustainable Chemistry*, vol. **6** (2023).  
<https://doi.org/10.1016/j.crgsc.2023.100365>
- [14] M. S. Lopes, M. E. Carneiro, A. V. Bento, D. C. Potulski, and G. I. B. De Muniz, Production and characterization of nanofibrillated cellulose powder, *Sci For*, vol. **49**, no. 129, (2021).  
<https://doi.org/10.18671/scifor.v49n129.04>
- [15] X. Liu, H. Sun, T. Mu, M. L. Fauconnier, and M. Li, Preparation of cellulose nanofibers from potato residues by ultrasonication combined with high-pressure homogenization, *Food Chem*, vol. **413** (2023).  
<https://doi.org/10.1016/j.foodchem.2023.135675>
- [16] H. Chutia and C. Lata Mahanta, Properties of starch nanoparticle obtained by ultrasonication and high pressure homogenization for developing carotenoids-enriched powder and Pickering nanoemulsion, *Innovative Food Science and Emerging Technologies*, vol. **74**, no. 102822 (2021).  
<https://doi.org/10.1016/j.ifset.2021.102822>
- [17] M. A. F. Supian, K. N. M. Amin, S. S. Jamari, and S. Mohamad, Production of cellulose nanofiber (CNF) from empty fruit bunch (EFB) via mechanical method, *J Environ Chem Eng*, vol. **8**, no. 1, (2020).  
<https://doi.org/10.1016/j.jece.2019.103024>
- [18] Q. Ji, X. Yu, A. E. G. A. Yagoub, L. Chen, and C. Zhou, Efficient cleavage of strong hydrogen bonds in sugarcane bagasse by ternary acidic deep eutectic solvent and ultrasonication to facile fabrication of cellulose nanofibers, *Cellulose*, vol. **28**, no. 10, pp. 6159–6182 (2021). <https://doi.org/10.1007/s10570-021-03876-w>
- [19] F. Fahma *et al.*, Nanocellulose-based fibres derived from palm oil by-products and their in vitro biocompatibility analysis, *Journal of the Textile Institute*, vol. **111**, no. 9, pp. 1354–1363 (2020).  
<https://doi.org/10.1080/00405000.2019.1694353>
- [20] X. Li, J. Li, Y. Kuang, S. Guo, L. Mo, and Y. Ni, Stabilization of Pickering emulsions with cellulose nanofibers derived from oil palm fruit bunch, *Cellulose*, vol. **27**, no. 2, pp. 839–851 (2020) <https://doi.org/10.1007/s10570-019-02803-4>
- [21] M. Poletto, H. L. Ornaghi Júnior, and A. J. Zattera, Native cellulose: Structure, characterization and thermal properties, *Materials*, vol. **7**, no. 9, pp. 6105–6119 (2014).  
<https://doi.org/10.3390/ma7096105>
- [22] Y. Peng, Y. Han, and D. J. Gardner, Spray drying cellulose nanofibrils: effect of drying process parameters on particle morphology and size distribution, *Wood and fiber science*, vol. **44**, no. 4, pp. 448–461, (2012)
- [23] W. Li, J. Yue, and S. Liu, Preparation of nanocrystalline cellulose via ultrasound and its reinforcement capability for poly(vinyl alcohol) composites, *Ultrason Sonochem*, vol. **19**, no. 3, pp. 479–485 (2012).  
<https://doi.org/10.1016/j.ultsonch.2011.11.007>
- [24] K. Zhang, Y. Su, and H. Xiao, Preparation and Characterization of Nanofibrillated Cellulose from Waste Sugarcane Bagasse by Mechanical Force, *Bioresources*, vol. **15**, no. 3, pp. 6636–6647, (2020).
- [25] M. R. Furtado, V. M. da Matta, C. W. P. Carvalho, W. L. E. Magalhães, A. L. Rossi, and R. V. Tonon, Characterization of spray-dried nanofibrillated cellulose and effect of different homogenization methods on the stability and rheological properties of the reconstituted suspension, *Cellulose*, vol. **28**, no. 1, pp. 207–221 (2021). <https://doi.org/10.1007/s10570-020-03516-9>
- [26] S. S. Lal and S. T. Mhaske, TEMPO-oxidized cellulose nanofiber/kafirin protein thin film crosslinked by Maillard reaction, *Cellulose*, vol. **26**, no. 10, pp. 6099–6118 (2019).  
<https://doi.org/10.1007/s10570-019-02509-7>

- [27] M. L. Nelson, Relation of Certain Infrared Bands to Cellulose Crystallinity and Crystal Lattice Type. Part I. Spectra of Lattice Types I, II, III and of Amorphous Cellulose, *J of Polym Sci. Vol 8*, pp 1311-1324 (1964).
- [28] A. Kljun, T. A. S. Benians, F. Goubet, F. Meulewaeter, J. P. Knox, and R. S. Blackburn, Comparative analysis of crystallinity changes in cellulose I polymers using ATR-FTIR, X-ray diffraction, and carbohydrate-binding module probes, *Biomacromolecules*, vol. **12**, no. 11, pp. 4121–4126, (2011).  
<https://doi.org/10.1021/bm201176m>
- [29] D. Koutsianitis *et al.*, Properties of ultrasound extracted bicomponent lignocellulose thin films, *Ultrason Sonochem*, vol. **23**, pp. 148–155, (2015).  
<https://doi.org/10.1016/j.ultsonch.2014.10.014>
- [30] R. Rotaru, M. E. Fortună, E. Ungureanu, and C. O. Brezuleanu, Effects of Ultrasonication in Water and Isopropyl Alcohol on High-Crystalline Cellulose: A Fourier Transform Infrared Spectrometry and X-ray Diffraction Investigation, *Polymers (Basel)*, vol. **16**, no. 16 (2024).  
<https://doi.org/10.3390/polym16162363>